Journal of Magnetism and Magnetic Materials 67 (1987) 123–129
North-Holland, Amsterdam

^{57}Fe HYPERFINE INTERACTION PARAMETERS AND SELECTED MAGNETIC PROPERTIES OF HIGH PURITY $MFe_{12}O_{19}$ (M = Sr, Ba)

B.J. EVANS [1], F. GRANDJEAN [2], A.P. LILOT [2], R.H. VOGEL [1] and A. GÉRARD [2]

[1] *Department of Chemistry, The University of Michigan, Ann Arbor, MI 48109, USA*
[2] *Institut de Physique, B5, Université de Liège, Sart Tilman, 4000 Liège 1, Belgium*

Received 31 March 1986; in revised form 20 October 1986

Much of the confusion regarding the ^{57}Fe Mössbauer spectroscopic hyperfine parameters of $SrFe_{12}O_{19}$ and $BaFe_{12}O_{19}$ at 300 K has been removed by means of an interlaboratory investigation of well-characterized samples prepared from high purity starting materials. In contrast to previous investigations, the contributions of each of the five Fe sublattices to the Mössbauer spectrum are discernible at 300 K and five components are necessary for an adequate fit of the data. The relative magnitudes of the hyperfine fields, H_n, and isomer shifts, δ, are as follows: for $SrFe_{12}O_{19}$ and $BaFe_{12}O_{19}$: $H_n(2b) < H_n(12k) < H_n(4f_1) < H_n(2a) < H_n(4f_2)$, for $SrFe_{12}O_{19}$ $\delta(4f_1) \leq \delta(2b) < \delta(12k) < \delta(2a) < \delta(4f_2)$, and for $BaFe_{12}O_{19}$ $\delta(2b) < \delta(4f_1) < \delta(12k) < \delta(4f_2) < \delta(2a)$. The above assignment is based on considerations of both magnetic and crystal/chemical structures.

The high purity starting materials seem to have appreciable influences on both hyperfine interaction parameters and bulk magnetic properties as observed by others for spinel and garnet ferrites.

1. Introduction

The hexagonal ferrites, $MFe_{12}O_{19}$ (M = Ba, Sr, Pb), with the magnetoplumbite structure type continue to be important permanent magnet materials in microwave, small motor, and, more recently, magnetic recording applications [1–3]. Important material parameters, in these applications are, inter alia, the bulk spontaneous magnetization and its temperature dependence. The bulk spontaneous magnetization is the resultant of the magnetizations of the individual sublattice of which there are five in the M-type hexaferrites. The various sublattices (iron sites) and the relative orientations of their spin moments are shown in table 1.

In contrast to simple spinel ferrites, the bulk magnetization of the M-type hexagonal ferrites exhibits an unusualy large, negative temperature coefficient [4]. As this large temperature coefficient places significant limitations on the applications of the M-type hexaferrites, an understanding of how it is related to the sublattice magnetizations and hyperfine fields is desirable.

Recent structural investigations of the M-type hexagonal ferrites and of the individual structural subunits [5,6] indicate that accurate interpretation of well-resolved ^{57}Fe Mössbauer spectra can lead to considerable advances in our understanding of

Table 1
Hyperfine parameters for $SrFe_{12}O_{19}$ (1)

Site and spin orientation	Laboratory	H_n [a] (kOe)	δ [a] (mms^{-1})	Δ [a] (mms^{-1})	Intensity
12k ↑	A	416	0.35	0.615	12
	B	411	0.34	0.61	12
$4f_1$ ↓	A	492	0.26	0.20	4.4
	B	492	0.30	0.38	4
$4f_2$ ↓	A	520	0.365	0.29	4
	B	516	0.42	0.47	4
2a ↑	A	507	0.34	0.10	2.4
	B	505	0.45	0.26	2
2b ↑	A	410	0.29	2.25	1.4
	B	411	0.33	2.29	2

[a] Estimated errors in H_n, δ relative to Fe metal and Δ are: ±4 kOe, 0.01 mms^{-1} and 0.05 mms^{-1}, respectively.

these structures and the relationship between the structure and bulk magnetic properties.

Unfortunately, there is considerable controversy regarding the hyperfine fields H_n of the five sublattices [7–12]. The divergences in the reported values of H_n are such that little can be said about the contributions of the different sublattices to the overall spontaneous magnatization. For example, the spread in reported values for some of the five sublattices approaches 100 kOe or about 25% of the average value of the sublattice hyperfine field [8,9]. A critical analysis of the reported data would lead to an immediate rejection of some of the hyperfine field values but some ambiguities in the existing data could not be resolved without further investigations. This investigation has been undertaken in order to resolve the controversy or to understand, at least, the basis of the ambiguities in the hyperfine interaction parameters of $SrFe_{12}O_{19}$.

Examination of the published ^{57}Fe Mössbauer spectra of barium and strontium M-type hexaferrites indicated that several factors could be contributing to the poor agreement among different investigators. The following are considered to be important: 1) differences in samples resulting either from different compositions, different synthesis conditions or both; 2) differences in methods of spectra analysis; and 3) differences in Mössbauer spectrometers. To obviate the controversies arising from the above three factors, an interlaboratory investigations has been undertaken.

Well-characterized specimens of barium and strontium M-type hexaferrites, i.e., $BaFe_{12}O_{19}$ and $SrFe_{12}O_{19}$, were prepared and exchanged between the two labortories. Spectra were acquired on different laboratory spectrometers and analyzed independently with different least-squares fitting programs; this was followed by a comparison of the spectra and data analysis. The interlaboratory comparison has been made primarily on $SrFe_{12}O_{19}$. Additional measurements were made on $BaFe_{12}O_{19}$ in only one of the laboratories and good concordance of the fitted hyperfine interaction parameters with those of $SrFe_{12}O_{19}$ did not warrant a detailed interlaboratory comparison. Much of the controversy regarding the ^{57}Fe hyperfine parameters of $BaFe_{12}O_{19}$ and $SrFe_{12}O_{19}$ has been resolved.

In order to have a comparison between the bulk magnetic properties and microscopic parameters of samples having well-characterized chemical compositions and hyperfine interaction parameters, spontaneous magnetization and the parameters of the B–H hysteresis loop have also been determined.

2. Experimental

The sample preparation and characterization have been described in detail [12,13]. Samples of $BaFe_{12}O_{19}$ and $SrFe_{12}O_{19}$ (1) were prepared from high purity (Johnson-Matthey Puratronic Grade 1) Fe_2O_3 (99.999%), $SrCO_3$ (99.994%) or $BaCO_3$ (99.999%). The powders were mixed in the form of an alcohol slurry in an agate ball-mill, dried, calcined at 1000 K, ball-milled, pressed into a pellet, weighed and fired in air at temperatures between 1073 and 1273 K for a period of 96 h. Each sample was subjected to repeated firing and ball-milling until a single phase was obtained as determined by X-ray powder diffractometry. Wet chemical analysis of $SrFe_{12}O_{19}$ by a commercial laboratory gave an Fe composition of 62.96% weight percent; the ideal stoichiometric value is 63.11 weight percent. X-ray powder diffraction patterns were obtained using CuKα radiation and a Norelco diffractometer equipped with a scintillation counter. Silicon was used as an internal standard. The lattice constants obtained are a = 0.5881 nm and c = 2.3026 nm which are in good agreement with the most recently published values of a = 0.58868 nm and c = 2.3037 nm [14] which were obtained, however, on a sample of unknown purity.

The Mössbauer spectrometer in laboratory A was of the constant acceleration type with an asymmetric (sawtooth) velocity waveform and with the spectrum being recorded in 512 channels. A 50 mCi ^{57}Co source in a rhodium matrix was employed as a source. The Mössbauer spectrometer in laboratory B was of the constant acceleration type with a symmetric (triangle) velocity waveform. The source was a 25 mCi ^{57}Co source dif-

fused in a rhodium matrix. The spectra were recorded in 400 channels.

The general method of computer-fitting the spectra in laboratory A has been described before [15,16]. Only the features particularly relevant to the hexagonal ferrite spectra are presented here. For each pattern the magnetic hyperfine field, H_n, electric quadrupole shift, ϵ, and isomer shift, δ, were free variables during the fitting. The different component patterns were assumed to be symmetric about their respective centers of gravity, and only three independent linewidths, Γ, and two intensities, I, parameters were employed for each 6-line patterns according to the following constraints: $\Gamma_i = \Gamma_{6-i}$; $I_i = I_{6-i}$ and $I_3 = 0.33 I_1$ where the subscripts refer to the line numbers in a single six-line pattern. The total number of fitted parameters was equal to 40.

In laboratory B, the fitting procedure was as follows: For each of the five Zeeman patterns, the fitted parameters were: the hyperfine magnetic field, H_n, the quadrupole splitting $\Delta = e^2Qq/2$, the isomer shift, δ, the angle θ between the hyperfine field and the principal axis of the electric field gradient (efg) tensor, the asymmetry parameter, η, of the efg tensor, the linewidth at half-maximum Γ, and the total intensity I. This gave a maximum number of adjustable parameters equal to 35. For each sublattice, the Hamiltonians of the ground and excited states were solved and Lorentzian lines were computed and added for the different transitions. The least-squares fit procedure is based on an algorithm described by Marquardt [17]. For $SrFe_{12}O_{19}$, the best fit was obtained with the following conditions. The relative population of each sublattice and, consequently, the relative intensity of each subspectrum was set equal to the site multiplicity (cf. table 1); the linewidth at half-height was set equal to 0.32 mms^{-1}. For symmetry reasons, the asymmetry parameter, η, was kept equal to 0 for all sites and the angle θ was allowed to differ from 0 only for the 12k site. These conditions reduced the total number of free parameters to 18. The MISFIT [10] goodness-of-fit parameter was used to judge the adequacy of both fitting procedures and ranged from 0.010 to 0.015, values which indicate excellent fits for these complex spectra.

Bulk magnetic measurements of M-ferrites were performed with a vibrating sample magnetometer of the Foner type [18]. The room temperature specific magnetization was measured in a maximum field of 10 kOe. Measurements on three samples are reported here: high purity $SrFe_{12}O_{19}$ (sample number 1), $SrFe_{12}O_{19}$ (sample number 2) studied previously and the high purity $BaFe_{12}O_{19}$ sample.

3. Results

^{57}Fe Mössbauer spectrum at 300 K of $SrFe_{12}O_{19}$ (1) is shown in fig. 1. The solid line is the result of a least-squares fit as performed in laboratory A. The ^{57}Fe hyperfine parameters obtained at 300 K in both laboratories are given in table 1. The hyperfine fields are in excellent agreement with the differences in magnitudes being less than the experimental error of approximately 1%.

The isomer shifts as determined in laboratory A follow the sequence $4f_2 > 12k > 2a > 2b > 4f_1$ whereas the sequence as determined in laboratory B is $2a > 4f_2 > 12k > 2b > 4f_1$. The rankings of

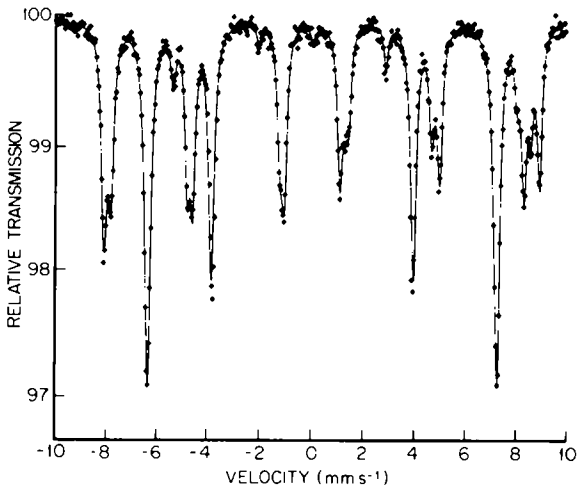

Fig. 1. ^{57}Fe Mössbauer spectrum of a high purity $SrFe_{12}O_{19}$ sample at 300 K. In the +7 to +10 mms^{-1} interval of the spectrum, components of all five sublattices can be observed: three components appear as well-resolved individual lines and two occur as shoulders.

the relative isomer shifts obtained in the two laboratories are in good agreement, with only one site, 2a, occupying different positions in the two determinations. This site, however, has one of the lowest intensities and would exhibit, in any case, parameters with large uncertainties in their values.

The agreement among the values for Δ is excellent for the 12k and 2b patterns because of the high intensity of the 12k pattern and the large magnitude of Δ for 2b; Δ can be determined with the greatest accuracy for these two patterns. The other patterns are rather insensitive to the value of Δ due to the poor resolution of the patterns and the smallness of the magnitude of Δ. For example, the shift in the positions of the outermost lines of the $4f_1$, $4f_2$ and 2a patterns as a result of the electric quadrupole interaction is less than 3% of their positions for a Δ of zero. Changes in the positions of the inner four lines are similar for either a non-zero electric quadrupole interaction or a non-zero isomer shift. It is noteworthy that divergences in the Δ values obtained in the two laboratories are accompanied by similar divergences in isomer shifts and represent intrinsic difficulties in fitting these complex and poorly-resolved spectra.

Even though the intensity parameters were treated in rather different ways in the two schemes of data analysis, it is not believed that the differences in intensity lead to any appreciable discrepancies; for example, the 2b intensities show the greatest differences (table 1) but the agreement of the hypefine field and electric quadrupole interaction is among the best shown for any site.

The ^{57}Fe Mössbauer spectrum of $BaFe_{12}O_{19}$ was also recorded and analyzed. It is very similar to that of $SrFe_{12}O_{19}$ and the hyperfine parameters are reported in table 3 for comparison with $SrFe_{12}O_{19}$.

The bulk magnetic measurements on two samples of $SrFe_{12}O_{19}$ and one sample of $BaFe_{12}O_{19}$ are reported in table 2: the saturation magnetization, σ_s, the remanent magnetization, σ_r, the coercive field, H_c, and the demagnetization energy $(BH)_{max}$ were deduced from the hysteresis loop. Fig. 2 shows, for instance, the hysteresis loop of $SrFe_{12}O_{19}$ (1). For comparison, some values from the literature are also reported in table 3.

Table 2
Average hyperfine parameters for $SrFe_{12}O_{19}$ and $BaFe_{12}O_{19}$

Site and spin orientation	Structural subunit	M	H_n [a] (kOe)	δ [a] (mms^{-1})	Δ [4] (mms^{-1})
12k ↑	R–S	Sr	414	0.345	0.612
		Ba	414	0.35	0.76
$4f_1$ ↓	S	Sr	492	0.28	0.29
		Ba	492	0.31	0.40
$4f_2$ ↓	R	Sr	518	0.395	0.38
		Ba	517	0.44	0.40
2a ↑	S	Sr	506	0.385	0.18
		Ba	511	0.45	0.20
2b ↑	R	Sr	411	0.31	2.27
		Ba	406	0.20	2.30

[a] Parameter errors are as in table 1.

Table 3
Bulk magnetic measurements of $MFe_{12}O_{19}$, M = Sr or Ba

M	Sample	σ_s (G cm^3 g^{-1})	σ_r (G cm^3 g^{-1})	H_c (Oe)	$(BH)_{max}$ (MGOe)
Sr	1	78.5	31	3500	4.3
	2	84.9		1290	
	ref. C			3000	4
	ref. SB	74.3			
Ba		75.8		2900	
	ref. H			4000	3-4
	ref. SB	72			

[C] A. Cochartd, J. Appl. Phys. 34 (1963) 1273.
[SB] B.T. Shirk and W.R. Buessem, J. Appl. Phys. 40 (1969) 1294.
[H] C. Heck, Magnetic Materials and their Applications, ed. Crane (Rusak, New York, 1974).

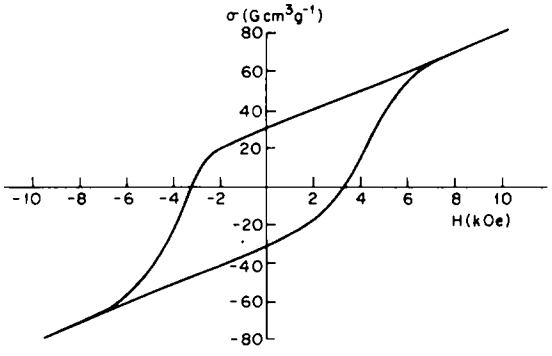

Fig. 2. $B-H$ hysteresis loop of $SrFe_{12}O_{19}$ at 283 K.

4. Discussion

For magnetic applications, the hyperfine fields of the various iron sublattices are the most important parameters and the agreement between the two laboratories on their values is quite good. For $SrFe_{12}O_{19}$, the magnitudes of H_n for 2b and 12k are so similar that they are virtually indistinguishable within the experimental error of Mössbauer spectroscopy. For $BaFe_{12}O_{19}$, a consideration of the available data from NMR experiments at ≈ 100 K [19] and of the current Mössbauer investigation leads us to conclude that at 300 K, the difference between H_n at the 12K and 2b sites is statistically significant.

Thus, the relative magnitudes of H_n at the five Fe sublattices appear to be well-established for the pure end-member compositions, $BaFe_{12}O_{19}$ and $SrFe_{12}O_{19}$. Further confirmation of the assignment of H_n to the various sublattices may be obtained from a consideration of the other hyperfine interaction parameters.

For example, the systematics of the isomer shifts and of the hyperfine fields at the octahedral and tetrahedral sites in spinel oxides are well established with the result that $\delta(\text{oct}) > \delta(\text{tet})$ and $H_n(\text{oct}) > H_n(\text{tet})$ at ~ 300 K. The M-type hexaferrites may be considered to consist of two crystallographic units [4,20]: an R block with the composition MFe_6O_{11} and an S block with the composition Fe_6O_8. The S block is a fragment of the spinel structure. Thus, in principle, the isomer shifts of the components of the Mössbauer spectra should constitute a reliable basis for assigning the different spectral components to the Fe sublattices. In the M-type hexaferrites, the $4f_1$ tetrahedral sites and 2a octahedral sites are located within the S block; the 2b and $4f_2$ octahedral sites are located within the R block. The 12k octahedral sites are located in the interface between the R and S block; 6 of these sites are derived from the S block and 6 are derived from the R block.

Therefore, we expect the isomer shift of the Fe^{3+} ($4f_1$) to be smaller than that of the Fe^{3+}(2a). Because $4f_1$ and 2a are entirely within the spinel block, we also expect H_n (2a) to be greater than $H_n(4f_1)$. The isomer shift of Fe^{3+} (12k) is also expected to be greater than that for $Fe^{3+}(4f_1)$ and to be very similar to that for Fe^{3+}(2a). Because 12k is not entirely within the spinel block, the magnitude of its hyperfine field relative to $4f_1$ and 2a cannot be easily predicted. The following sequence of isomer shifts and magnetic hyperfine fields is therefore predicted without any ambiguity: $\delta(2a) \gtrsim \delta(12k) > \delta(4f_1)$ and $H_n(2a) > H_n(4f_1)$ and is, indeed, observed in $BaFe_{12}O_{19}$ and $SrFe_{12}O_{19}$ (table 2).

The situation with respect to the hyperfine parameter of the Fe sites in the R block is quite different from that in the spinel block as there are no well-established systematics for Fe^{3+} having similar local crystal chemistries and magnetic spin and exchange interactions. Nevertheless, it has been argued that for a given coordination polyhedron the isomer shift is proportional to the Fe^{3+}–O^{2-}-internuclear separation [21]. The $4f_2$ Fe^{3+}–O^{2-} internuclear separation is greater than that for 2a (table 4) and $\delta(4f_2)$ is, therefore, expected to be greater than δ(2a), as observed.

As in the case of the other R block Fe sites, little can be said that is definitive regarding the relative magnitude of H_n for the $4f_2$ site.

There are no comparison data for either δ or H_n for the trigonal bipyramidal Fe^{3+} 2b site. However, as there is a general correlation between coordination number and isomer shift, we might expect the isomer shift of Fe^{3+}(2b) to occupy an intermediate position between those of Fe^{3+}(12k) and $Fe^{3+}(4f_1)$. But in this case, the general correlation between isomer shift and coordination number for Fe^{3+} oxides should be applied with

Table 4
Internuclear Fe^{3+}–O^{2-} distances in $BaFe_{12}O_{19}$

Site	Fe^{3+}–O^{2-} distance (10^{-8} cm)		Isomer [a] shift (mms^{-1})
	Townes et al. [11]	Obradors et al. [12]	
2b	2.060 [b] (10)	2.039 [b] (3)	0.31
12k	2.023 (5)	2.028 (3)	0.35
$4f_2$	2.018 (8)	2.021 (3)	0.40
$4f_1$	1.916 (10)	1.894 (3)	0.28
2a	1.995 (6)	2.000 (2)	0.39

[a] Isomer shifts in $SrFe_{12}O_{19}$ at 298 K relative to Fe metal.
[b] Based on a dynamic model of disorder in which the 2b Fe ions occupy one or another of the local minima on each side of the equatorial plane of the "trigonal bipyramidal" site.

caution as there is no significant change in internuclear separation in going from the octahedral to the trigonal bipyramidal site in $MFe_{12}O_{19}$ (table 4). Therefore, the relative values of the isomer shift at the 2b site cannot be predicted with confidence. Thus, it is perhaps fortuitous that $\delta(2b)$ is smaller than $\delta(4f_2)$ in both compounds. Furthermore, these relative values of δ may not be due entirely to static bonding effects as $\delta(2b)$ is certainly reduced to some extent at 300 K by the large second-order Doppler shift as a result of its dynamic motion across the equatorial plane of the trigonal bipyramid [22]. As shown in table 2, the 2b site isomer shift of $BaFe_{12}O_{19}$ (0.20 mms^{-1}) is significantly smaller than the 2b site isomer shift of $SrFe_{12}O_{19}$ (0.31 mms^{-1}). This difference may be related to the crystallographic and chemical environment of the 2b site. Indeed, as the 2b site is the closest to the M^{2+} ions, it is expected to be strongly influenced by the nature of the M^{2+} ions [18].

While it is clear that these are some Intrinsic limitations in the precision with which the ^{57}Fe hyperfine interactions of the hexagonal ferrites can be determined, the systematic of the relative magnitude of these parameters and their interrelationships as outlined above should be of considerable value in investigations of heavily substituted materials.

From the macroscopic magnetic data reported in table 3, it can be seen that $SrFe_{12}O_{19}$ (1) exhibits a demagnetization energy of 4.3 MGOe, which is rather large for a sample in which no deliberate attempt was made to enhance the energy product and is believed to be related to the use of high purity starting materials. A similar influence of high purity starting materials on the bulk magnetic properties of YIG and Ni-Ferrites has been observed recently [23]. The differences in the bulk magnetic properties of $SrFe_{12}O_{19}$ (1) and $SrFe_{12}O_{19}$ (2) may be understood in terms of differences in the granularity of both samples. The average diameter of the grains of $SrFe_{12}O_{19}$ (1) is less than 38 μm whereas the diameter of the grains of $SrFe_{12}O_{19}$ (2) is less than 63 μm. Thus, the former one has a grain size closer to the single domain grain size (5 μm) and consequently shows a higher coercive field.

5. Conclusions

This interlaboratory investigation shows that samples of $SrFe_{12}O_{19}$ and $BaFe_{12}O_{19}$ prepared from high purity starting materials have superior magnetic properties and exhibit well-resolved Mössbauer spectra with all five Fe sublattices clearly visible. For both $SrFe_{12}O_{19}$ and $BaFe_{12}O_{19}$, the ranking of the hyperfine fields at 300 K for the five Fe sublattices was determined to be the same in both laboratories, i.e., $H_n(2b) < H_n(12k) < H_n(4f_1) < H_n(2a) < H_n(4f_2)$. For $SrFe_{12}O_{19}$, the sequence of relative values for the isomer shift was the same in both laboratories except for the position of the 2a site; for laboratory A the sequence is $\delta(4f_1) < \delta(2b) < \delta(2a) < \delta(12k) < \delta(4f_2)$ and for laboratory B, $\delta(4f_1) < \delta(2b) < \delta(12k) < \delta(4f_2) < \delta(2a)$. For $BaFe_{12}O_{19}$, the sequence of relative isomer shift values is found to be $\delta(2b) < \delta(4f_1) < \delta(12k) < \delta(4f_2) < \delta(2a)$ in laboratory B and is similar to that observed for $SrFe_{12}O_{19}$ except for the single reversal of the positions of the 2b and $4f_1$ sites.

The overall good agreement between the hyperfine parameters of $BaFe_{12}O_{19}$ and $SrFe_{12}O_{19}$ cannot be attributed to similar methods of data analysis or identical instrumental configurations as these were significantly different in the two laboratories. Consequently, these two factors cannot be responsible for the divergences in previously reported ^{57}Fe data obtained in different laboratories. Therefore, the poor agreement among the results of the earlier investigations is due primarily to differences in sample preparation or composition. An inspection of the published spectra clearly supports this conclusion; indeed, nominal $BaFe_{12}O_{19}$ and $SrFe_{12}O_{19}$ samples showed such remarkably different spectra that the samples must have been different in composition or in the phases present.

Acknowledgement

Partial support of this investigation by a NATO grant is gratefully acknowledged.

References

[1] A. Tucciarone, J. Magn. Magn. Mat. 20 (1980) 111.

[2] V. Enz, in: Ferromagnetic Materials, vol. 3, ed. W.P. Wohlfarth (North-Holland, Amsterdam, 1982) p. 3–35.

[3] M. NaOe, S. Hasunuma and S. Yamanaka, IEEE Trans. Magn. MAG-17 (1982) 3184.

[4] H. Kojima, in: Ferromagnetic Materials, vol. 3, ed. W.P. Wohlfarth (North-Holland, Amsterdam, 1982) p. 305–392.

[5] X. Obradors, A. Collomb, M. Pernet, D. Samaras and J.C. Joubert, J. Solid State Chem. 56 (1985) 171.

[6] M.C. Cadée and D.J.W. IJdo, J. Solid State Chem. 52 (1984) 302.

[7] G. Albanese, J. Phys. C1-38 (1977) C1-C85 and references therein.

[8] A.M. Van Diepen and F.K. Lotgering, J. Phys. Chem. Solids 35 (1974) 1641 and references therein.

[9] G.N. Belozerskii and Yu.P. Khimich, Sov. Phys. Solid State 17 (1975) 871.

[10] V. Florescu, D. Barb, M. Morariu and D. Tarina, Rev. Roum. Phys. 19 (1974) 249.

[11] P.M. Rao, A. Gerard and F. Grandjean, Phys. Stat. Sol. 54 (1979) 529.

[12] R.H. Vogel and B.J. Evans, J. Magn. Magn. Mat. 13 (1979) 294.

[13] R.H. Vogel, Ph.D. Thesis, University of Michigan (1981).

[14] M.C. Morris et al., NBS Monograph 25-Section 18, 69 (1981).

[15] B.J. Evans and G. Amthauer, J. Phys. Chem. Solids 41 (1980) 985.

[16] B.J. Evans, R.G. Johnson, F.E. Senftle, C.B. Cecil and F. Dulong, Geochimica et Comsochimica Acta 46 (1982) 761.

[17] D.W. Marquardt, J. Soc. Indust. Appl. Math. 11 (1963) 431.

[18] A.-P. Lilot, Ph.D. Thesis, Université de Liège (1983).

[19] R.L. Streever, Phys. Rev. 186 (1969) 285.

[20] P.H. Lacorre, M. Hervieu and B. Raveau, Rev. Inorg. Chem. 6 (1984) 195.

[21] R. Jagannathan and K.N. Shrisvastava, Hyperfine Interactions 7 (1979) 377.

[22] J.G. Rensen and J.S. Van Wieringen, Solid State Commun. 7 (1969) 1139.

[23] M. Guyot, V. Cagan and T. Merceron, IEEE Trans. Magn. MAG-20 (1984) 2157.